JGR Oceans

RESEARCH ARTICLE
10.1029/2021JC018039

Secular Variability of the Upwelling at the Canaries Latitude: An Instrumental Approach

D. Gallego[1], R. García-Herrera[2,3], E. Mohino[2], T. Losada[2], and B. Rodríguez-Fonseca[2,3]

[1]Departamento de Sistemas Físicos, Químicos y Naturales, Universidad Pablo de Olavide, Seville, Spain, [2]Departamento de Física de la Tierra y Astrofísica, Universidad Complutense, Madrid, Spain, [3]IGEO, Instituto de Geociencias (CSIC, UCM), Madrid, Spain

Key Points:

- Historical wind direction observations are used to build a centennial-long upwelling intensity series for the Canaries
- Upwelling at the Canaries shows trends highly dependent upon the period considered
- North Atlantic Sea Surface Temperatures drive the upwelling intensity at the Canaries at multidecadal scales

Correspondence to:
D. Gallego,
dgalpuy@upo.es

Citation:
Gallego, D., García-Herrera, R., Mohino, E., Losada, T., & Rodríguez-Fonseca, B. (2022). Secular variability of the upwelling at the Canaries latitude: An instrumental approach. *Journal of Geophysical Research: Oceans*, *127*, e2021JC018039. https://doi.org/10.1029/2021JC018039

Received 24 SEP 2021
Accepted 26 FEB 2022

Author Contributions:
Conceptualization: D. Gallego
Formal analysis: D. Gallego
Funding acquisition: R. García-Herrera
Investigation: D. Gallego, R. García-Herrera, E. Mohino, T. Losada, B. Rodríguez-Fonseca
Methodology: D. Gallego, R. García-Herrera, E. Mohino, T. Losada, B. Rodríguez-Fonseca
Project Administration: R. García-Herrera
Resources: R. García-Herrera
Software: D. Gallego
Supervision: R. García-Herrera
Validation: D. Gallego, E. Mohino, T. Losada, B. Rodríguez-Fonseca
Visualization: D. Gallego
Writing – original draft: D. Gallego

Abstract In this research we make use of historical wind direction observations to assemble an instrumental upwelling intensity index (the so-called Directional Upwelling Index [DUI]) for the coast of Northwest Africa between 26° and 33°N and from 1825 to 2014. The DUI is defined as the persistence of the alongshore winds at the coast and unlike other upwelling indices, it relies on observed wind direction solely, avoiding the suspected bias toward increasing wind speed of historical wind observations documented in previous research. We have found that between June and October, when the upwelling intensity in the area is at its seasonal maximum, the persistence of the north-easterlies measured by the DUI is significantly related to the alongshore wind stress and subsequently with Sea Surface Temperature anomalies at the coast of NW Africa. The analysis of the DUI record does not display a consistent long-term trend but an oscillatory behavior. At interannual time scales this variability can be linked to the changes in the strength and location of the subtropical north Atlantic high-pressure center and at multidecadal scales, the upwelling seems mainly driven by the Atlantic Multidecadal Variability through the modulation exerted by this climatic pattern on the intensity of the Saharan low.

Plain Language Summary Upwelling is a process in which sea water from intermediate depths rises toward the surface as a response to the wind friction along the west coast of continents. Upwelled water is rich in nutrients, creating areas of paramount importance for fisheries. A long-standing hypothesis contends that upwelling might be intensified because of global warming, but due to the impediments to quantify the upwelling intensity for long periods, the scientific community still debates whether the upwelling is changing. We have used historical wind observations taken aboard ships sailing along the coast of Northwest Africa to show that there, during the last two centuries, upwelling has not increased but it has oscillated synchronically with the temperature of the North Atlantic.

1. Introduction

The Canary Upwelling System (CUS) extends from the coast of West Africa, approximately at 10°N, to the coast of Galicia in northern Spain, around 45°N (Arístegui et al., 2009). North of 15°N the shelf is relatively narrow and the main modulator of the upwelling intensity is the Ekman transport driven by the alongshore component of the wind (Cropper et al., 2014; Sylla et al., 2019). The associated pumping of cool and nutrient-rich sea water toward the ocean surface is of paramount importance for fisheries (Brochier et al., 2018), so the description of the upwelling interannual variability and the search of long-term trends associated with global warming have become relevant subjects (Barange et al., 2018). However, the quantification of these parameters is challenging and historically, different analyses result in contradictory conclusions (Barton et al., 2013). The lack of agreement mostly comes from the nature of the observations necessary to quantify the upwelling intensity (Jacox et al., 2018). Upwelling is usually determined by the Sea Surface Temperature (SST) gradient between coastal waters and open ocean (Benazzouz et al., 2014; Cropper et al., 2014; Narayan et al., 2010). This requires the use of satellite-derived high-resolution SST fields, limiting the length of the series. On the other hand, as stationary winds blowing along the coast toward the equator enhance the westward Ekman mass transport, wind-derived indices are also widely used to quantify coastal upwelling, especially when the length of the series is relevant (Barton et al., 2013; Gómez-Gesteira et al., 2008; Santos et al., 2012; Sylla et al., 2019). These dynamical indices are typically based on historical reanalysis, which strongly rely on International Comprehensive Ocean-Atmosphere Data Set (ICOADS) data (Freeman et al., 2017; Wohland et al., 2019). It is believed that ICOADS' wind velocities are biased toward increased values (Barton et al., 2013), most probably due to the shift from estimated to

Writing – review & editing: R. García-Herrera, E. Mohino, T. Losada, B. Rodríguez-Fonseca

anemometer-measured winds and the changes in the interpretation of the Beaufort scale along the time (Gallego et al., 2007; Thomas et al., 2008). Because of this, there have been no attempts to use ICOADS-dependent datasets to develop upwelling indices prior to the 1950s decade (Sydeman et al., 2014).

In a recent paper, Gallego et al. (2021) demonstrated that to evaluate the upwelling intensity at the coasts of Senegal and Mauritania, the biases on the wind velocity could be sidestepped by using only wind direction observations. By developing what these authors called a "directional upwelling index [DUI]," they were able to study the variability of the upwelling intensity at the southern end of the CUS for almost 200 years.

Further north, between 26° and 33°N, along the coasts of Morocco and through the Canaries, upwelling has a very different regime, being strongly modulated by the mid-latitude circulation. Upwelling at this latitude is accompanied by the southward branch of the subtropical gyre, namely the offshore Canary current (Sylla et al., 2019). There, upwelling is maximum between June and October following both the migration and seasonal strengthening of the Azores High and the intensification of the Saharan low (Soares et al., 2019). In this region, upwelling is usually restricted to the first tens of km from the coast, where SSTs are on average 3°C–4°C colder than in open sea during the peak of the upwelling season in August (Figure 1a).

Remarkably, along these waters, historically there have been an intense traffic of ships covering the maritime route between Europe and Asia or South America resulting in thousands of early in-situ observations of wind direction going back to the beginning of the nineteenth century. In this paper, we analyze the upwelling intensity at the latitude of the Canary Islands between June and October by applying the technique developed in Gallego et al. (2021).

2. Data and Method

2.1. Data

To characterize the upwelling at the Canaries' latitude by means of a directional index, we used the box (26°–33°N; 24°W–9°W) (CAN area in successive, black rectangle in Figures 1a–1c). Within this area, our main source of wind direction records has been ICOADS (3.0 release, see Freeman et al., 2017). Figure 1b shows the density of observations, being the predominant ship's routes well inside the selected box. To complement the ICOADS data, we searched for undigitized wind direction observations at the NW coast of Africa at the UK National Archives at Kew ("Cape, West Africa & St. Helena" series; AMD 51 and AMD 52). We focused on the 1800–1900 period and in the range of latitudes between 5° and 45°N. We abstracted a total of 67,339 new wind direction observations, with the maximum density of observations clearly following the predominant route of British ships toward Southern Africa in the nineteenth century (Figure 1c).

Figure 1d shows the evolution of the total number of wind direction observations from 1750 to 2014 inside CAN. Prior to 1850, the number of observations is below 1,000 per year. In 1854 a large increase in data availability is evident, first reaching over 1,000 observations per year. Along the mid-1880s, there is a second increase in data availability. Since that decade, the number of observations per year is almost continuously over 5,000, peaking over 30,000 by the late 1960s and throughout the 1970s. The exceptions are the evident drops in data availability during World War 1 and especially the years during and immediately after World War 2. It has been estimated that at monthly resolution, at least 10 observations per month on different days are necessary to compute a meaningful index (Gallego et al., 2015). This corresponds to a minimum of 120 observations per year, so the coverage attained at the CAN area allows the generation of directional indices starting around the 1820s decade, when the number of available annual observations first exceeds the 100 per year mark on a regular basis (Figure 1d).

Apart from raw wind direction observation, we make use of the National Centers for Environmental Prediction/National Center for Atmospheric Research (NCEP/NCAR) reanalysis 2 (Kanamitsu et al., 2002) and the daily Operational Sea Surface Temperature and Sea Ice Analysis (OSTIA) SST data between 1982 and 2014 at a resolution of 1/20° (Good et al., 2020). We make also use of the following climate indices: The North Atlantic Oscillation (NAO) instrumental index of Jones et al. (1997) from 1821 to 2014, the summer NAO index (Folland et al., 2009) from 1836 to 2014 and the Atlantic Multidecadal Oscillation (AMO) index (Enfield et al., 2001) from 1856 to 2014.

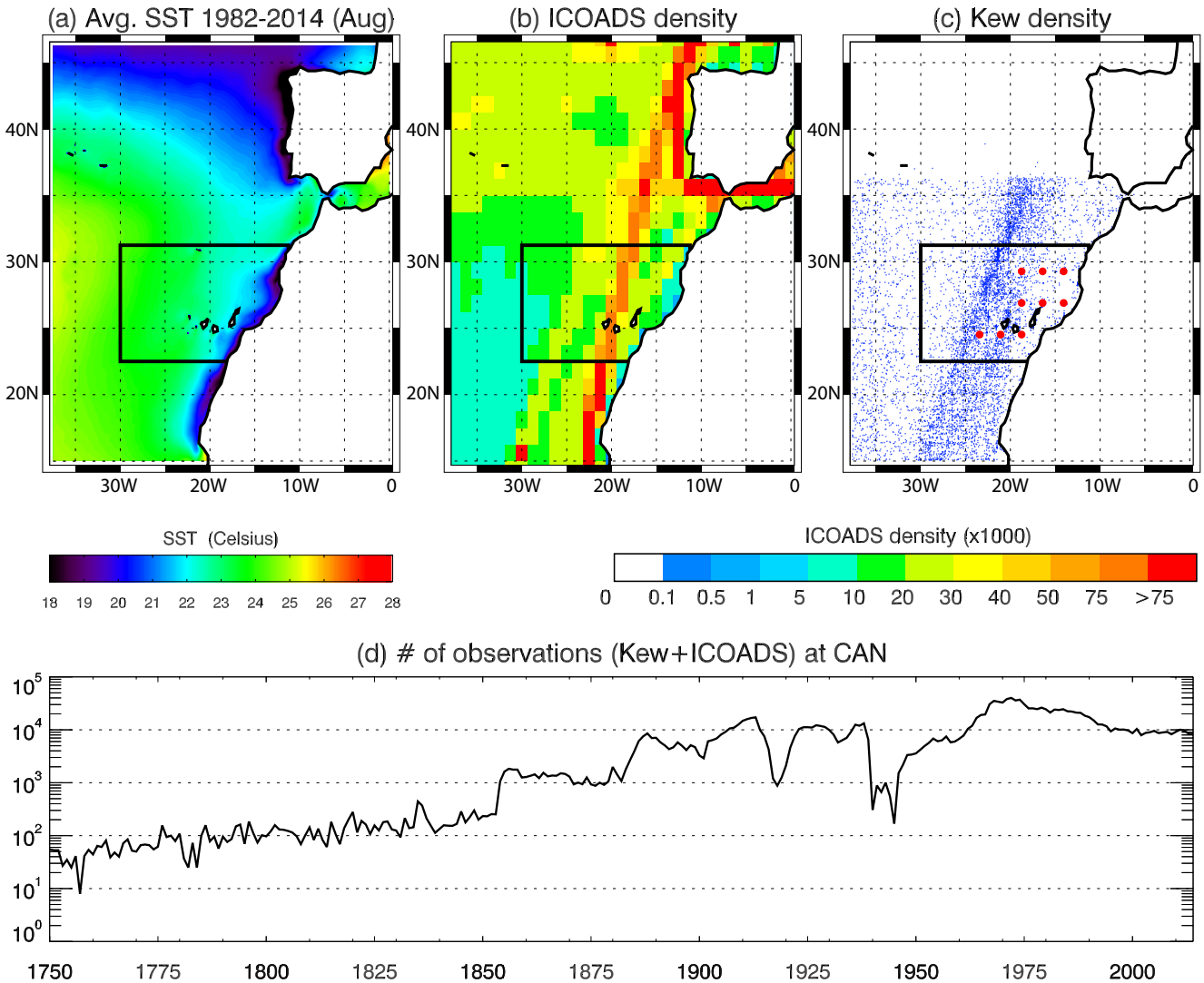

Figure 1. (a) Average August Sea Surface Temperature (SST) based on daily Operational Sea Surface Temperature and Sea Ice Analysis (OSTIA) SST data (Good et al., 2020) from 1982 to 2014. (b) International Comprehensive Ocean-Atmosphere Data Set (ICOADS) coverage in a 1° × 1° grid. (c) Wind direction observations taken from the Kew Archives for this research (blue dots), red dots indicate the grid-points used for calibration based on National Centers for Environmental Prediction/National Center for Atmospheric Research (NCEP/NCAR) reanalysis 2 momentum flux and (d) Evolution of the total (Kew + ICOADS) number of observations inside the CAN area used to compute the DUI. Black rectangles in (a), (b) and (c) define the CAN area.

2.2. Index Definition

The reader is referred to Gallego et al. (2021) for a complete description of the definition of a directional index applied to an upwelling system, here we give a summary of the methodology.

As the coast of NW Africa at the CAN latitude is roughly oriented in the NE direction, to quantify the persistence of the alongshore winds at the Canaries latitude we have defined the DUI as the percentage of days in a month with prevalent wind flowing from the NE inside CAN. A day has been considered of "prevalent wind flowing from the NE" when at least 91% of the total number of wind observations available that day report wind flowing from ±45° of the true NE direction. The 91% threshold was determined by a calibration procedure designed to maximize the correlation of the DUI with the projection over the NE direction of the magnitude of the monthly mean of the momentum flux taken from the NCEP/NCAR reanalysis 2 and averaged over the three grid points closest to the coast within the CAN area (red dots in Figure 1c). The period for calibration was 1982–2014 and the average correlation between the DUI and the NCEP/NCAR NE momentum flux between June and October for this period resulted in $r = +0.69$ ($p < 0.01$).

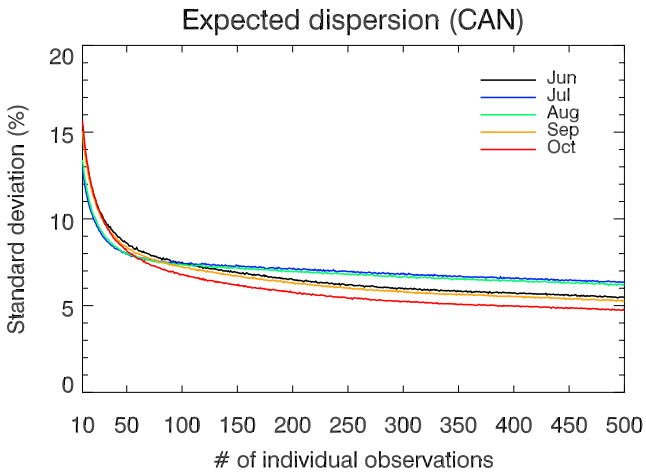

Figure 2. Expected dispersion (in %) of the DUI index computed from a given number of wind direction observations (*x*-axis) between June and October.

It must be stressed that by construction, we assume as equivalent any observation taken inside CAN. The spatial variability of the wind inside this area over 1 million km^2 is inevitably translated as uncertainty in a particular realization of the index, as separate subsets of observations could led to a different value of the DUI. Quantifying the significance of this effect is crucial to understand the DUI variability, as changes in the preferent routes followed by the ships could be translated as spurious trends in the DUI not necessarily related to climate. In this sense, within the CAN area there are two main routes followed by the ships. The route from Europe to Central and South Africa is the most frequent. It corresponds to the maxima in ICOADS density that crosses the Canaries (Figure 1b). However, in the nineteenth century, the routes starting in Europe and aimed to South America were also relevant. They ran slightly westward of the previous one (secondary maxima in data density in Figure 1b). This evolution of the preferent route was very gradual but it constitutes a good example of how the spatial distribution of the wind observations within CAN changed along the decades and could be translated as non-climatic signal in the DUI. To estimate the expected dispersion of the index due to sampling differences, we adopted a bootstrap approach as in Gallego et al. (2015). For every year and month between 1971 and 2010, 1,000 "degraded" DUIs were constructed from a number "*N*" of randomly selected wind observations, with N ranging from 10 to 500. This period was selected because for these years, ICOADS has the greatest data density, essentially covering all the study area. The average standard deviation of these 1,000 degraded DUIs as a function of N can be interpreted as the sampling-induced uncertainty of the DUI computed from a given number of observations (Figure 2). As expected, the largest standard deviations are found for indices computed with fewer observations (around 13%–16% for $N = 10$). This value rapidly decreases as N increases, as the sampling becomes more representative of the entire area. For $N = 50$ observations, the standard deviation is below 10% in all cases and by $N = 150$, the deviation is always below 8%, slowly decreasing as N increases. The fact that the standard deviation does not tend to zero reflects the inherent spatial variability of the wind within CAN.

3. Results

3.1. Relation of the DUI With the Wind Stress and the SSTs

Figure 3 shows the seasonal cycle of the momentum flux used as calibrator (red dashed line) and the evolution of the calibrated DUI (black line). The seasonal evolution of the alongshore momentum flux is well captured by the DUI. Both the DUI and the NE momentum flux are minimum between November and February. During these months the DUI is below 20% (less than 20% of the days in these months are characterized by prevailing

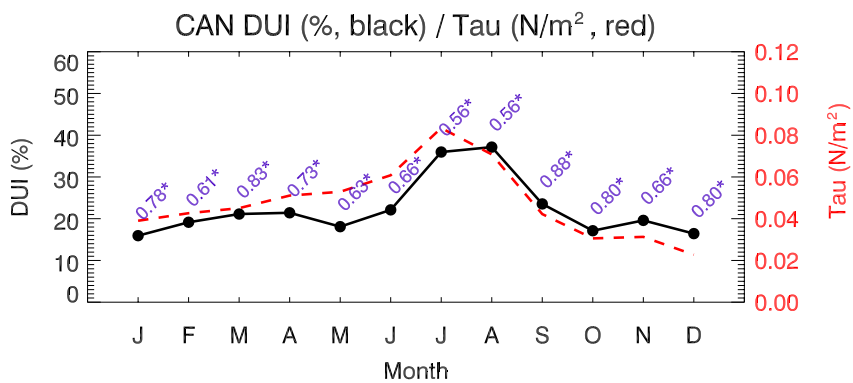

Figure 3. Monthly values of the National Centers for Environmental Prediction/National Center for Atmospheric Research (NCEP/NCAR) reanalysis 2 momentum flux projected in the NE direction and averaged over the three grid points closer to the coast within the CAN box (red dashed line) and DUI in % (Black line). Blue numbers indicate the correlation between both series for the calibration period 1982–2014. Asterisks mark values statistically significant at the $p < 0.05$ level.

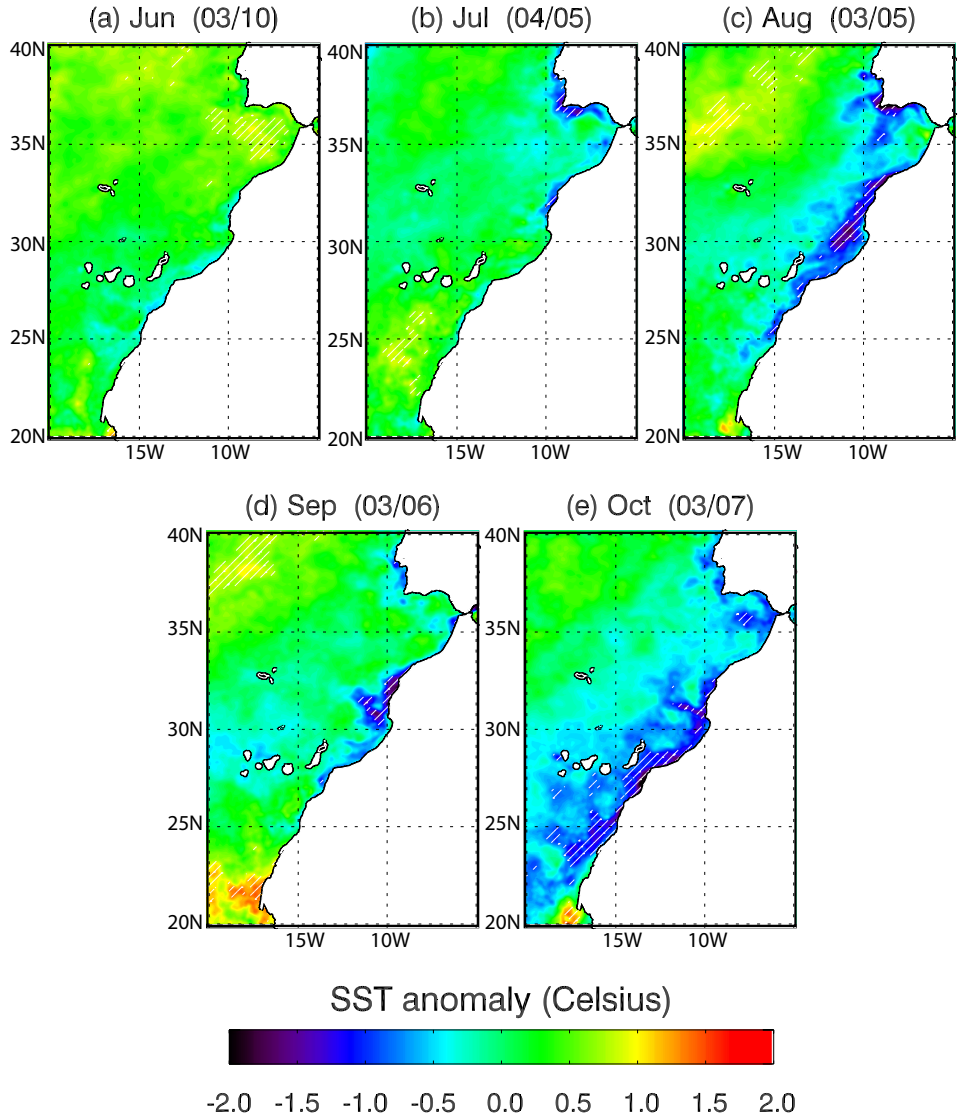

Figure 4. Difference between the monthly average Sea Surface Temperature (SST) data from the Operational Sea Surface Temperature and Sea Ice Analysis for the years in which the DUI is over the 90% percentile minus the years with DUI below the 10% percentile over the period 1982–2014. Numbers over each case indicate the number of cases over the 90% percentile/below the 10% percentile included in each composite. Hatched areas indicate significant differences based on a 1,000-trial bootstrap procedure.

winds flowing from the NE inside the CAN box) and the NE momentum flux close to the African coasts ranges from 0.023 $N{\cdot}m^{-2}$ in December to 0.043 $N{\cdot}m^{-2}$ in February. Maximum values of the DUI and the NE momentum flux are reached in July (37.2% and 0.083 $N{\cdot}m^{-2}$ respectively) and August (37.2% and 0.071 $N{\cdot}m^{-2}$). Even more relevant that the correct reproduction of the seasonal evolution are the values of the correlation between the DUI and the NE momentum flux (blue numbers in Figure 3). These correlations are statistically significant ($p < 0.05$) all year round and they range from $r = +0.56$ in July and August to $r = +0.88$ in September.

Regarding the DUI signature on the SST variability, Figure 4 shows the difference between the monthly average SST for the years when the DUI is over the 90% percentile minus the years with DUI below the 10% percentile over the period 1982–2014 covered by the OSTIA SSTs. The results show a consistent enhancement of the coastal upwelling during years of large DUI although the intensity of the anomalies is monthly dependent. In June and July, at the beginning of the upwelling season the changes are moderate. In June (Figure 4a) the cold tongue is apparent at the Canaries latitude, but the SST anomaly is rather small, with values that do not exceed

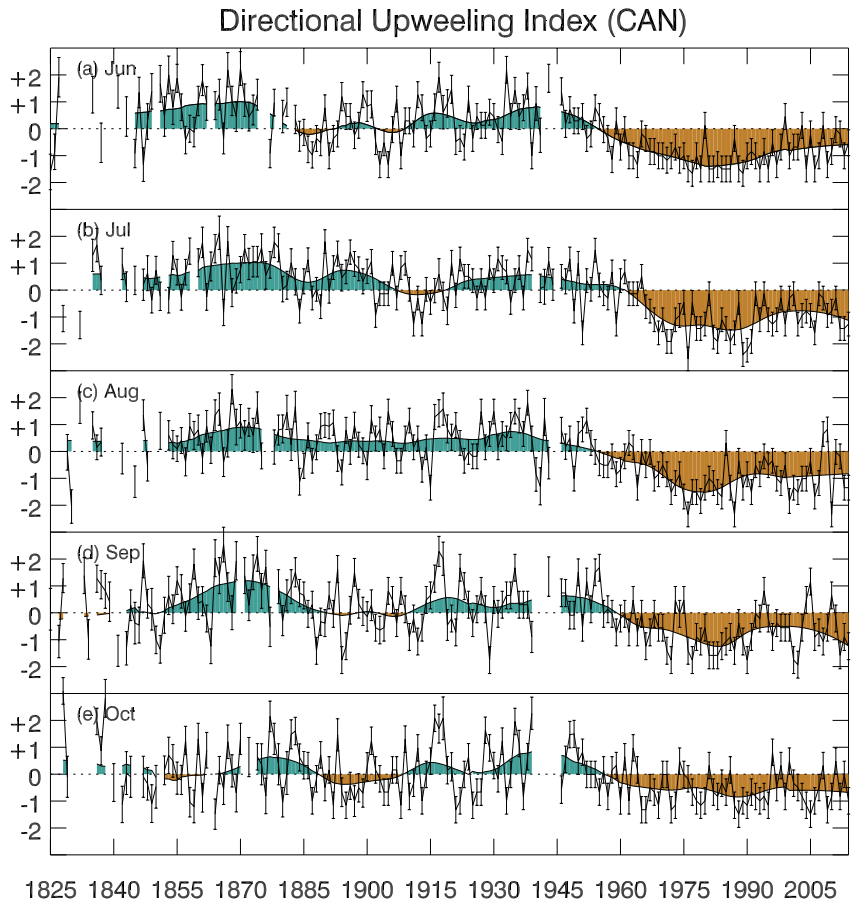

Figure 5. Standardized DUI from June to October between 1825 and 2014. Error bars indicate the expected standard deviation based on the number of observations available each year as described in the main text. Shaded curve represents a robust locally weighted regression with a 31-year window.

−0.5°C. In July, a clearer upwelling enhancement is evident above 21°N (Figure 4b), being statistically significant ($p < 0.05$). By August, at the core of the upwelling season, the enhancement of the cold surge associated with DUI anomalies is already evident along the entire coast of NW Africa (Figure 4c) with temperature anomalies around −1.5°C. This signal is also clearly seen in September and especially October (Figures 4d and 4e). It must be pointed out that the DUI signature on temperature is not restricted to extreme cases, as the same pattern is obtained when the DUI is regressed on the SSTs (figure not shown).

3.2. DUI Temporal Evolution

Figure 5 shows the time series of the monthly DUI from June to October (black line). To ease comparison among different months, the standardized values relative to the 1825–2014 period have been represented. Error bars correspond to the expected dispersion based on the number of available observations in each case (see Figure 2). The shaded curve represents a locally weighted scatterplot smoothing performed with a 31-year window width. This averaging method is comparable to a running mean but provides a robust estimation of the long-term changes of time series with missing intervals (Cleveland, 1979).

In general, the DUI is highly variable at the sub-decadal time scale, with noticeable fluctuations of variable periodicity. In all months, the period between 1825 and 1875 was characterized by notable higher than average DUI values. During the eight decades between the late 1870s and the 1950s the DUI values are closer to the long-term average and for some months and specific periods, lower than average values are seen, especially between the late nineteenth century and the first 15 years of the twentieth century However, the most striking characteristic of the DUI is the relatively fast drop to lower-than-average values evidenced at the end of the 1950s. This shift

is independently observed for all months. However, it must be stressed that although in the entire 1825–2014 perspective the years since the late 1950s show frequent cases of lower-than-average DUI, within the period 1960–2014, the DUI shows alternating trends. This is quite evident between July and September (Figures 5b–5d).

The overall trend of the monthly DUIs for the entire 1825–2014 period is statistically significant ($p < 0.01$) and negative in all months (titles in Figure 6) ranging between −0.12%/yr in October and −0.23%/yr in July. However, these global trends seems a consequence of the tendency of the DUIs to be over/below their long-term averages at the beginning/end of the study period. A running analysis reveals that the DUI's trends are very dependent upon the specific period considered (shading in Figure 6). Although with some differences among the five analyzed months, in general the period 1850–1870 was characterized by a slight increasing trend in the DUI, which was followed by a period of negative trend between 1870 and 1885. Between 1885 and 1945, alternating changes in the trend of the DUI are seen for all months, although a general positive but not statistically significant trend in the DUI is seen for large windows and all months in this period. The large drop in the DUI values occurring around the late 1950s, is seen in Figure 6 as a large and consistent negative trend in the DUI which started around 1950 and lasted up to the first half of the 1970s decade. This negative trend is significant for all months and window widths. In general, from the late 1970s and up to the end of the series in 2014, the trend in the DUI has remained mainly, but not exclusively positive, especially in the period from the late 1980s and the 1990s.

3.3. The Role of the Atlantic Climate Modes

It is commonly accepted that the AMV, typically quantified by the Atlantic multidecadal oscillation index (AMO) and the NAO must exert some control on the upwelling variability at NW Africa (Bonino et al., 2019; Narayan et al., 2010; Pardo et al., 2011). Previous research faced the problem with relatively short observational series, limiting the significance of their results. Subsequent analysis have used modeled data rather than direct observations, especially at the time of studying multidecadal variability (Bonino et al., 2019). The length of the DUI series offers for the first time, the opportunity of studying the relation of the upwelling variability at NW Africa and these global climate modes for a period of over a century, relying solely on observational data.

In this section we will concentrate on the core of the upwelling season at NW Africa so we will consider the July to September (JAS) averages of the NAO and AMO indices. It is interesting to point out that during the summer, the centers of action of the North Atlantic SLP dipole are noticeably displaced toward the northeast in relation to their winter-autumn counterparts. This makes "traditional" NAO indices, especially those computed from SLP observations on fixed locations, scarcely representative of the variability of the North Atlantic dipole in summer (Bladé et al., 2012). Therefore, we also included in this analysis the summer variant of the NAO index (SNAO) which is defined as the first empirical orthogonal function of summertime extratropical North Atlantic pressure at mean sea level (Folland et al., 2009). With this definition, a positive phase of the SNAO implies an anomalous displacement of the subtropical high over northwestern Europe and the British Isles while the negative phase implies a deeper southward- and eastward-displaced Iceland low (Folland et al., 2009).

Figure 7 shows the sliding correlations for the period 1825–2014 between the DUI and the NAO, the SNAO and the AMO for windows of variable width. The NAO shows mainly positive correlations with the DUI (i.e., stronger subtropical high implying enhanced upwelling-favorable winds), but in general, the correlations are low, unstable, and only statistically significant in the 1970s and for short periods. However, this lack of correlation seems mostly a consequence of the inability of the NAO index at the time of characterizing the changes in the location of the subtropical high-pressure center during the summer. In this sense, the DUI-SNAO correlations are clearly more stable than those of the NAO. These correlations are mostly negative and statistically significant for large periods of the twentieth century but for a 30-year interval between the 1930s and the late 1950s. This indicates that during the summer, the anomalous displacement (relative to its average location in summer) of the subtropical high-pressure center toward northwestern Europe associated to the positive phases of the SNAO implies a consistent decrease in the intensity of the upwelling-favorable trade wind along the coasts of Morocco. This effect had been previously detected by Bladé et al. (2012) although at the time, it was not related to the upwelling at the CAN (see for example Figure 10 in Bladé et al., 2012).

Regarding the AMO (Figure 7c), the correlations are highly variable. For short windows, the correlation alternates in sign, although they are not statistically significant. Interestingly, for longer windows, two extended periods of positive correlation are evidenced, which reach statistical significance in the case of the periods

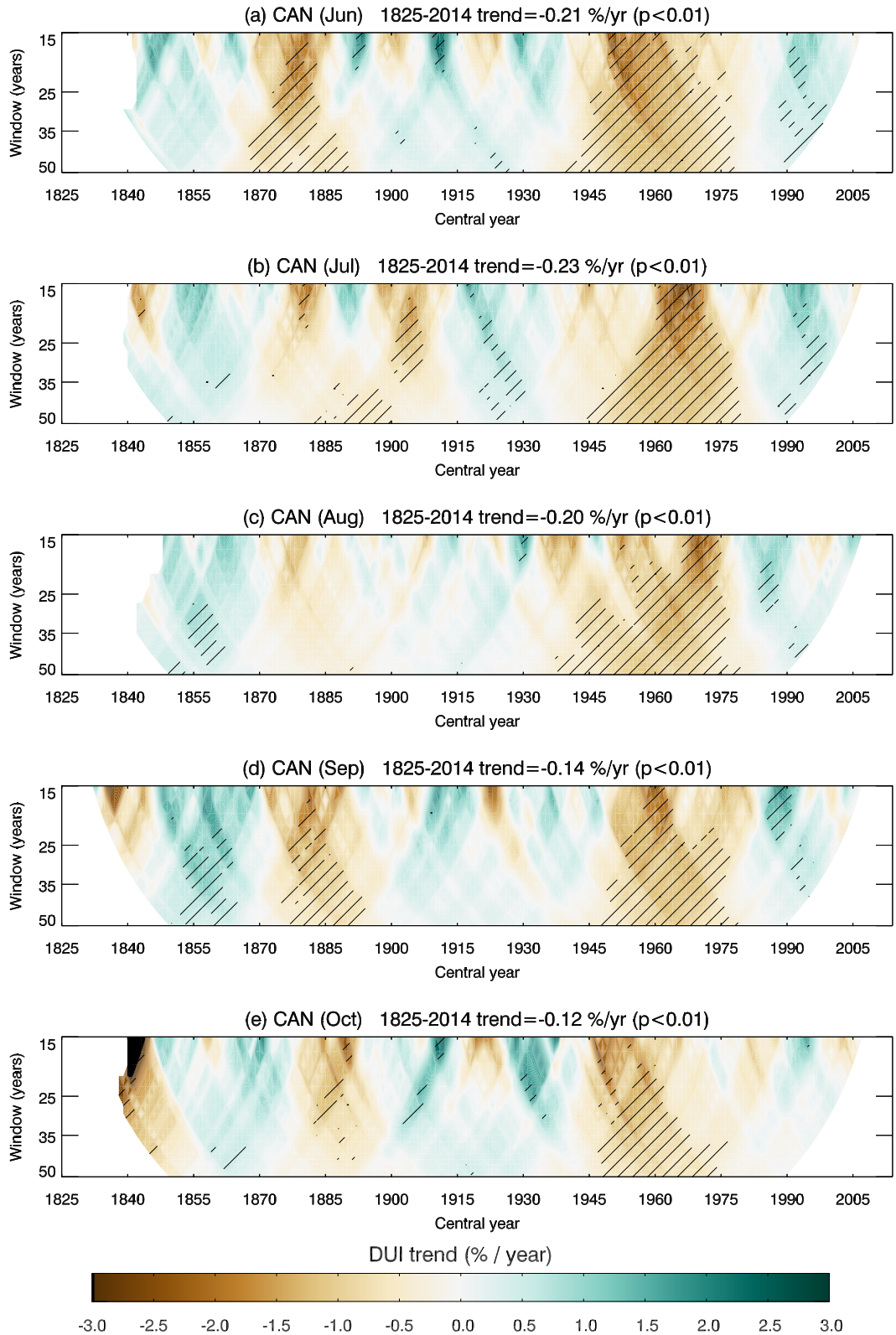

Figure 6. Linear trends of the DUI in % per year for a sliding window centered at the year indicated on the *x*-axis and width indicated on the *y*-axis. Hatched areas indicate statistically significant trends at $p < 0.05$. *x*-axis is escalated as in Figure 5 to ease comparison.

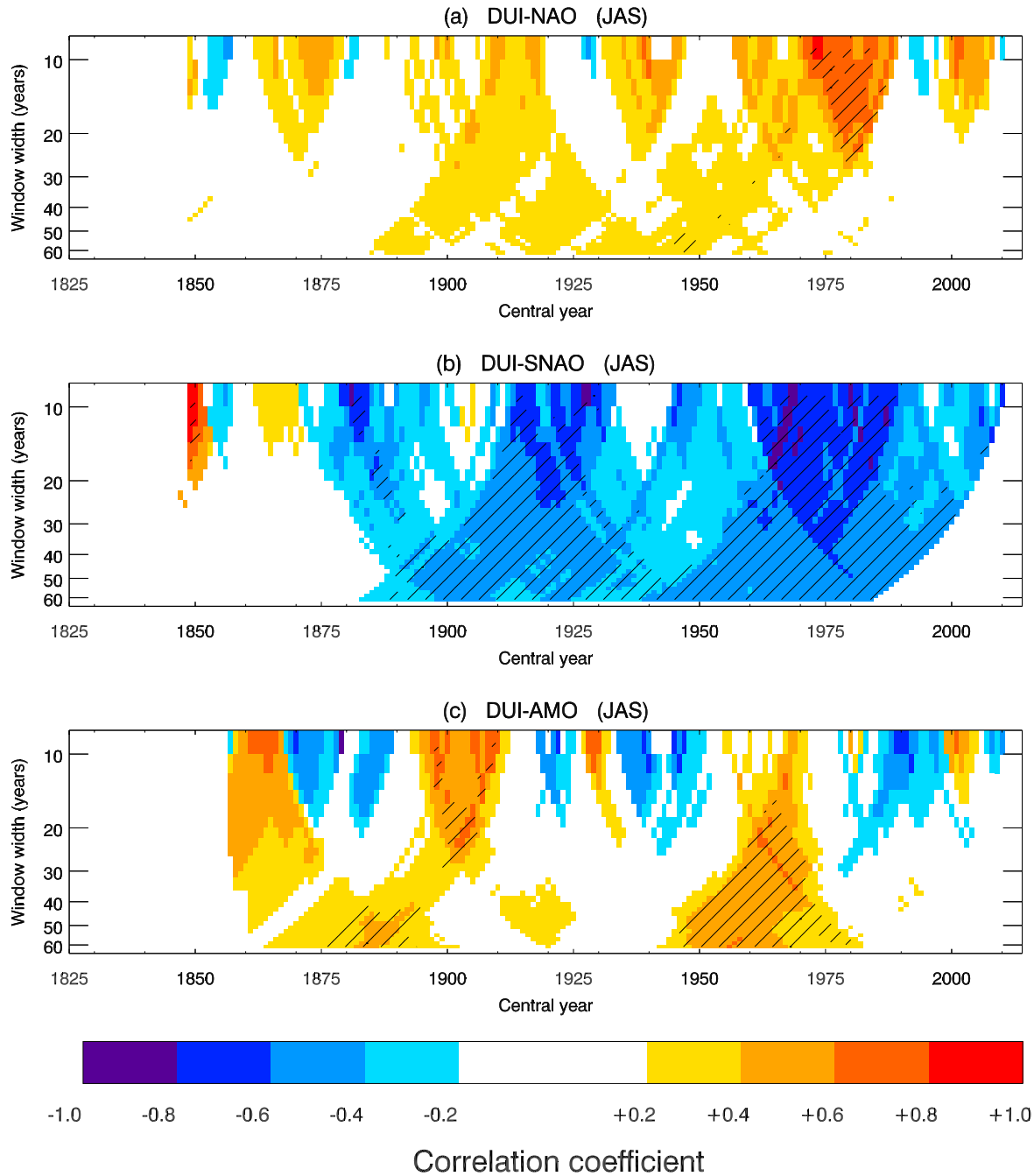

Figure 7. Running Pearson's correlation coefficient for variable window width (*y*-axis) between the July to September average Directional Upwelling Index (DUI) and (a) the North Atlantic Oscillation (NAO) index (b) the Summer North Atlantic Oscillation (SNAO) index and (c) the multidecadal oscillation index (AMO). Hatched areas indicate statistically significant correlation at $p < 0.05$.

1870–1890 and 1950–1980. This constitutes a striking result, as it is contrary to the relation usually accepted between the AMO phase and the occurrence of upwelling favorable winds at the Canaries latitude. In general, it is assumed that the lower SSTs in the North Atlantic during AMO negative phases is accompanied by an enhanced subtropical high and therefore an increase the upwelling favorable winds at the Canaries (Alexander et al., 2014; Marrero-Betancort et al., 2020; Pardo et al., 2011). This relation would imply a negative correlation between upwelling favorable winds and the AMO index. Recently, Bonino et al. (2019) found this negative correlation to be significant, supporting this paradigm. However, in our analysis we found mainly positive correlations, strongly suggesting that warmer/colder North Atlantic tends to be concurrent with favorable upwelling winds during the

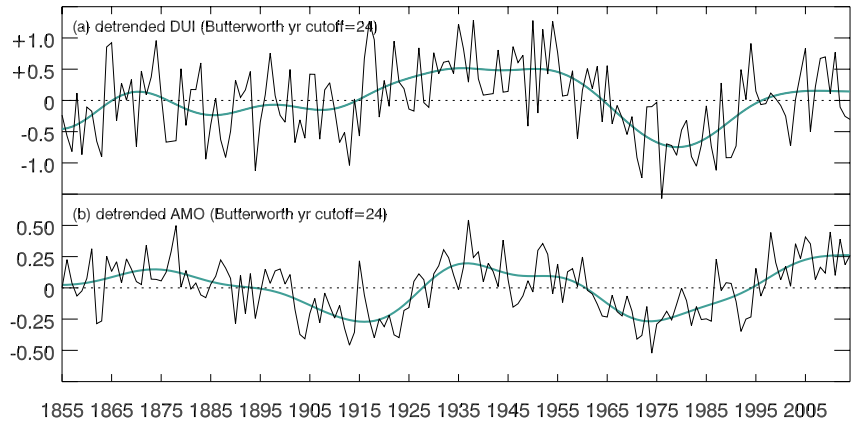

Figure 8. (a) Standardized and detrended low pass filtered JAS Directional Upwelling Index (DUI) and (b) standardized and detrended low pass filtered Atlantic Multidecadal Oscillation (AMO). Black lines correspond to the unfiltered series.

summer, when the upwelling in this area is at its maxima. It is relevant to point out that this positive correlation only arises for the longest windows in Figure 7c, suggesting that the correlation between the AMO and the DUI is related to low frequency variability.

To analyze the relation between the DUI and the AMO at decadal and superior time scales we first detrended the JAS DUI and then applied a low-pass Butterworth filter with a 24-year cut-off frequency, which is roughly equivalent to a running mean with a 10-year window (Mohino et al., 2011). When the resulting series is compared to the equivalently filtered AMO, the similitude between the long-term evolution of the JAS-AMO and the JAS-DUI evolution over the last 160 years becomes evident (Figure 8). The correlation coefficient of the filtered series reaches $r = +0.57$ and it was found to be maximum for zero-lag (i.e., AMO and DUI are approximately in-phase). However, a random-phase test Ebisuzaki (1997) for this correlation resulted in a p value of 0.13 not reaching statistical significance.

4. Discussion

The length of the DUI record offers a new perspective on the long-term variability of the alongshore winds at the CUS and it allows to shed new light into one of the most controversial and still unresolved debates in climatology: the determination of the long-term trend in the upwelling at this region. Since the publication by Bakun (1990) of the "Upwelling Intensification Hypothesis" as a consequence of global warming, a lot of research has been undertaken in order to uncover this trend on observed or modeled data. However, the difficulties at the time of quantifying the upwelling intensity for long periods of time in this area have led to contradictory results. Several authors (Cropper et al., 2014; McGregor et al., 2007; Narayan et al., 2010; Wang et al., 2015) have reported evidence supporting the intensification proposed by Bakun. On the other hand, there are several studies reporting a decrease in the upwelling intensity (Barton et al., 2013; Gómez-Gesteira et al., 2008; Gómez-Letona et al., 2017; Sylla et al., 2019), the absence of significant trends (Mote & Mantua, 2002) or seasonal dependent trends (Sousa et al., 2017). Therefore, the question of whether the CUS is increasing or not is clearly far from being resolved (Barton et al., 2013).

In general, our results indicate that the upwelling favorable winds at CAN have not experienced a steady trend. Although for the entire period 1825–2014 the overall trend of the DUI is negative, there is an evident oscillatory behavior, with the DUI remaining over/below its long-term mean for prolonged periods of time. This implies the existence of periods with trends of alternating sign, as shown in Figure 6. In this regard, the DUI tended to be steadily over the mean from 1825 to 1875, and below it from 1960 to the present time with a noticeable shift to lower values occurring in a relatively short period of time between the early 1950s and the early 1970s. After the large shift to lower-than-average values occurred between the 1950s and the 1970s, the DUIs display a clear recovery toward larger values during the last years of the twentieth century and the first decade of the 21st century. Such an increase would support Bakun's hypothesis. However, the DUI record also shows that there have been other periods with similar upward trends in the DUI, as it was the case of the years between the late 1840s

and 1870 or the first two decades of the twentieth century (see Figures 5c and 5d for example), periods with small anthropogenic influence on global climate. This result does not discard the influence of global warming on the upwelling trend, but does not seem to support a consistent connection of global warming with an increase of the upwelling favorable wind stress, at least at CAN.

Similarly to the trend issue, there is no agreement on the role of major climate modes in the modulation of the upwelling at NW Africa. In general, it is admitted that upwelling-favorable winds off NW Africa, must be linked to the NAO and the AMV. The NAO influence would be driven by changes on the location and strength of the North Atlantic subtropical high. However, published literature reports very low upwelling-NAO correlations (Narayan et al., 2010; Pardo et al., 2011) and the cases in which some significant correlations are found (e.g., Cropper et al., 2014; Marrero-Betancort et al., 2020) are referred to the winter-spring months, while for the summer, when coastal upwelling at the CAN is most relevant, they report non-significant correlations. In this sense, the NAO indices used in previous literature might not be optimal to study the North Atlantic circulation influence on the upwelling at the CAN. Our DUI correlates poorly with the historical NAO index by Jones et al. (1997) in summer as well. However, when the SNAO index (Folland et al., 2009) is used, the correlation largely increases and attains statistical significance for large periods of the twentieth century, indicating that in summer, the interannual variability in the position and strength of the subtropical High represented by the SNAO do have a noticeable effect on the upwelling intensity at the CAN latitude.

Concerning the relation with the AMV, which is typically assessed by correlating the DUI with the AMO index, its effect on the upwelling has been even more elusive than that of the NAO. Narayan et al. (2010) considered the effect of the AMV as insignificant, disregarding any primary control of this pattern over the intensity of coastal upwelling off NW Africa. Subsequently, several papers (Alexander et al., 2014; Marrero-Betancort et al., 2020; Pardo et al., 2011) found some evidence that a negative phase of the AMO should imply enhanced upwelling-favorable winds at NW Africa. Recently Bonino et al. (2019) found this negative correlation to be significant using a modeled upwelling index at the Canaries supporting this scheme, and linked it to the modulation of the inter-hemispheric meridional gradient of SST and SLP over the Atlantic basin exerted by the AMV. On the contrary, we have found positive correlations (warmer North Atlantic implying more frequent upwelling favorable winds) for the months of maximum upwelling at NW Africa (July to September). This positive correlation becomes especially evident for the low pass filtered series. Although the positive correlation for the filtered series does not reach statistical significance because of the reduction in the degrees of freedom of the statistical contrast associated to the low-pass filtering (Ebisuzaki, 1997), Figure 8 clearly shows that the low-pass filtered detrended JAS DUI tends to follow rather closely the evolution of the AMO along the entire study period. The reason for the discrepancy in the sign of the correlation in relation with previous works relies on the different months considered. In our analysis we focus on summer. This is quite relevant, as the wind anomalies related to opposite phases of the AMO at NW Africa are strongly dependent upon the season. In this sense, as shown by Martin and Thorncroft (2014) during autumn, winter, and most of spring, a positive AMO phase is concurrent to upwelling unfavorable wind anomalies at the CAN latitude related to a weaker subtropical high, in good accordance with the negative correlations found between the AMO and wind-derived upwelling indices computed in annual or multi-seasonal averages in previous research. However, in summer, the effect of the enhancement of the Saharan low on the alongshore winds at NW Africa would become relevant (see Figure 7 in Martin & Thorncroft, 2014). In this season, a positive phase of the AMO would imply an enhanced Saharan low, contributing to an increase of the NE upwelling favorable winds at the NW African coast resulting in the positive correlation found between the DUI and the AMO. To assess this hipotesis, we made an analysis analogous to that of Figure 4 but for the NCEP/NCAR SLP. We found a thermal low 1–2 hPa deeper for months with large DUIs (figure not shown), strongly suggesting that the changes in the SLP over Northern Africa do play a significant role in the upwelling variability at the CAN latitude.

Finally, we consider interesting to point out that while the AMV effect on the wind circulation at the CAN latitude is elusive, this is not the case for the AMV modulation of other relevant wind system at NW Africa as it is the West Africa Monsoon (WAM), a modulation also deeply related with the strength of the Saharan low (Berntell et al., 2018; Haarsma et al., 2005; Martin & Thorncroft, 2014). During the boreal summer, the WAM is characterized by south-westerly winds that blow from the ocean between latitudes 9°N and 20°N bringing the seasonal rains to the Sahel area. The AMV influence on the intensity of this monsoon is currently well established. Warm phases of the AMO involve an anomalous low centered over the northeast Sahara (Haarsma et al., 2005) that

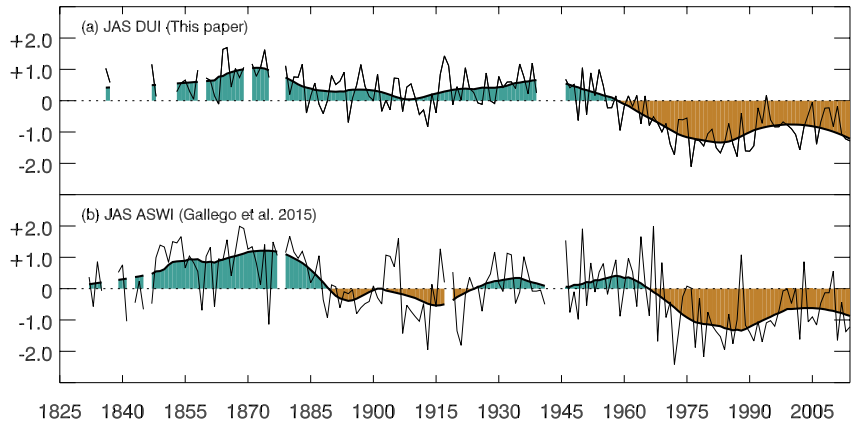

Figure 9. (a) July to September average of the standardized DUI and (b) July to September average of the African Southwesterly Index (ASWI) by Gallego et al. (2015). The ASWI is a direct measure of the intensity of the West African Monsoon. Shaded curves represent a robust locally weighted regression with a 31-year window as in Figure 5.

increases the moisture flux convergence toward the Sahel thus increasing monsoonal rains (Berntell et al., 2018). Therefore, during the summer, and according to the results presented in this paper, the AMV should drive both the WAM and the upwelling-favorable wind intensity at the CAN latitude measured by the DUI in the same sense through the changes induced in the Saharan low. In this regard, Gallego et al. (2015) developed a directional index analogous to the DUI but aimed to quantify the WAM intensity (the so-called ASWI, see Figure 9a) offering the possibility of comparing the century-long evolution of the WAM strength and the upwelling favorable winds at the CAN latitude by relying on a consistent observational data set and a common methodology, an infrequent opportunity for this region of the world as recently pointed out by Berntell et al. (2018). When the DUI and the ASWI are compared (Figure 9), the similarity between them is evident, supporting the idea of a common driver for both wind systems acting at the multidecadal scale.

Summing up, our results indicate that the upwelling favorable winds at CAN are very variable. In summer, this variability can be linked to the changes in the location and the strength of the subtropical high measured by the SNAO index but especially to the changes in the SLP ocean-continent gradient related to the anomalies of the Saharan low, which is largely modulated by the AMV. In this sense, the AMV arises as a major modulator of the wind variability for the entire NW coast of Africa, impacting not only on the strength of the WAM or the Saharan low described in previous research, but also on the intensity of the alongshore upwelling favorable winds between 26° and 33°N.

Data Availability Statement

ICOADS data are provided by the U.S. National Oceanic and Atmospheric Administration and are available at https://icoads.noaa.gov/. NCEP_Reanalysis 2 data provided by the NOAA/OAR/ESRL PSL, Boulder, Colorado, USA, from their Web site at Operational Sea Surface Temperature and Ice Analysis data are provided by the Copernicus Marine Service (identifier SST_GLO_SST_L4_NRT_OBSERVATIONS_010_001). NAO index is provided by the Climatic Research Unit at https://crudata.uea.ac.uk/cru/data/nao/. SNAO index provided by the KNMI at https://climexp.knmi.nl/. AMO index provided by the NOAA/ESRL/PSD at http://www.esrl.noaa.gov/psd/data/timeseries/AMO/.

Acknowledgments
We thank Dr. Clive Wilkinson for his assistance with the UK National Archives collection. Esther González did intensive work abstracting logbooks. Research funded by the Spanish Ministerio de Economía y Competitividad under grant CGL2015-72164-EXP (UPNAO). E.M., T.L. and B.R. also thank the support of EU-TRIATLAS project (grant agreement 817578). Funding for open access publishing: Universidad Pablo de Olavide/CBUA.

References

Alexander, M. A., Halimeda Kilbourne, K., & Nye, J. A. (2014). Climate variability during warm and cold phases of the Atlantic Multidecadal Oscillation (AMO) 1871–2008. *Journal of Marine Systems*, *133*, 14–26. https://doi.org/10.1016/j.jmarsys.2013.07.017

Arístegui, J., Barton, E. D., Álvarez-Salgado, X. A., Santos, A. M. P., Figueiras, F. G., Kifani, S., et al. (2009). Sub-regional ecosystem variability in the Canary current upwelling. *Progress in Oceanography*, *83*(1–4), 33–48. https://doi.org/10.1016/j.pocean.2009.07.031

Bakun, A. (1990). Coastal ocean upwelling. *Science*, *247*(4939), 198–201. https://doi.org/10.1126/science.247.4939.198

Barange, M., T. Bahri, M. C. M. Beveridge, K. L. Cochrane, S. Funge-Smith, & F. Poulain (Eds.), (2018). *Impacts of climate change on fisheries and aquaculture: Synthesis of current knowledge, adaptation and mitigation options*. FAO Fisheries and Aquaculture Technical Paper No. 627.

Barton, E. D., Field, D. B., & Roy, C. (2013). Canary current upwelling: More or less? *Progress in Oceanography*, *116*, 167–178. https://doi.org/10.1016/j.pocean.2013.07.007

Benazzouz, A., Mordane, S., Orbi, A., Chagdali, M., Hilmi, K., Atillah, A., et al. (2014). An improved coastal upwelling index from sea surface temperature using satellite-based approach – The case of the Canary Current upwelling system. *Continental Shelf Research*, *81*, 38–54. https://doi.org/10.1016/j.csr.2014.03.012

Berntell, E., Zhang, Q., Chafik, L., & Körnich, H. (2018). Representation of multidecadal Sahel rainfall variability in 20th century reanalyses. *Scientific Reports*, *8*(1). https://doi.org/10.1038/s41598-018-29217-9

Bladé, I., Liebmann, B., Fortuny, D., & van Oldenborgh, G. J. (2012). Observed and simulated impacts of the summer NAO in Europe: Implications for projected drying in the Mediterranean region. *Climate Dynamics*, *39*(3–4), 709–727. https://doi.org/10.1007/s00382-011-1195-x

Bonino, G., Di Lorenzo, E., Masina, S., & Iovino, D. (2019). Interannual to decadal variability within and across the major eastern boundary upwelling systems. *Scientific Reports*, *9*(1). https://doi.org/10.1038/s41598-019-56514-8

Brochier, T., Auger, P.-A., Pecquerie, L., Machu, E., Capet, X., Thiaw, M., et al. (2018). Complex small pelagic fish population patterns arising from individual behavioral responses to their environment. *Progress in Oceanography*, *164*, 12–27. https://doi.org/10.1016/j.pocean.2018.03.011

Cleveland, W. S. (1979). Robust locally weighted regression and smoothing scatterplots. *Journal of the American Statistical Association*, *74*(368), 829–836. https://doi.org/10.1080/01621459.1979.10481038

Cropper, T. E., Hanna, E., & Bigg, G. R. (2014). Spatial and temporal seasonal trends in coastal upwelling off Northwest Africa, 1981–2012. *Deep Sea Research Part I: Oceanographic Research Papers*, *86*, 94–111. https://doi.org/10.1016/j.dsr.2014.01.007

Ebisuzaki, W. (1997). A method to estimate the statistical significance of a correlation when the data are serially correlated. *Journal of Climate*, *10*(9), 21472–22153. https://doi.org/10.1175/1520-0442(1997)010<2147:amtets>2.0.co

Enfield, D. B., Mestas-Nuñez, A. M., & Trimble, P. J. (2001). The Atlantic Multidecadal Oscillation and its relation to rainfall and river flows in the continental U.S. *Geophysical Research Letters*, *28*(10), 2077–2080. https://doi.org/10.1029/2000gl012745

Folland, C. K., Knight, J., Linderholm, H. W., Fereday, D., Ineson, S., & Hurrell, J. W. (2009). The summer north Atlantic oscillation: Past, present, and future. *Journal of Climate*, *22*(5), 1082–1103. https://doi.org/10.1175/2008jcli2459.1

Freeman, E., Woodruff, S. D., Worley, S. J., Lubker, S. J., Kent, E. C., Angel, W. E., et al. (2017). ICOADS release 3.0: A major update to the historical marine climate record. *International Journal of Climatology*, *37*(5), 2211–2232. https://doi.org/10.1002/joc.4775

Gallego, D., Garcia-Herrera, R., Calvo, N., & Ribera, P. (2007). A new meteorological record for Cádiz (Spain) 1806–1852: Implications for climatic reconstructions. *Journal of Geophysical Research*, *112*(D12). https://doi.org/10.1029/2007jd008517

Gallego, D., García-Herrera, R., Losada, T., Mohino, E., & Rodríguez de Fonseca, B. (2021). A shift in the wind regime of the southern end of the canary upwelling system at the turn of the 20th century. *Journal of Geophysical Research: Oceans*, *126*(5). https://doi.org/10.1029/2020jc017093

Gallego, D., Ordóñez, P., Ribera, P., Peña-Ortiz, C., & García-Herrera, R. (2015). An instrumental index of the West African Monsoon back to the nineteenth century. *Quarterly Journal of the Royal Meteorological Society*, *141*(693), 3166–3176. https://doi.org/10.1002/qj.2601

Gómez-Gesteira, M., de Castro, M., Álvarez, I., Lorenzo, M. N., Gesteira, J. L. G., & Crespo, A. J. C. (2008). Spatio-temporal upwelling trends along the canary upwelling system (1967-2006). *Annals of the New York Academy of Sciences*, *1146*(1), 320–337. https://doi.org/10.1196/annals.1446.004

Gómez-Letona, M., Ramos, A. G., Coca, J., & Arístegui, J. (2017). Trends in primary production in the canary current upwelling system—A regional perspective comparing. *Remote Sensing Models. Frontiers in Marine Science*, *4*. https://doi.org/10.3389/fmars.2017.00370

Good, S., Fiedler, E., Mao, C., Martin, M. J., Maycock, A., Reid, R., et al. (2020). The current configuration of the OSTIA system for operational production of foundation sea surface temperature and ice concentration analyses. *Remote Sensing*, *12*(4), 720. https://doi.org/10.3390/rs12040720

Haarsma, R. J., Selten, F. M., Weber, S. L., & Kliphuis, M. (2005). Sahel rainfall variability and response to greenhouse warming. *Geophysical Research Letters*, *32*(17). https://doi.org/10.1029/2005gl023232

Jacox, M. G., Edwards, C. A., Hazen, E. L., & Bograd, S. J. (2018). Coastal upwelling revisited: Ekman, Bakun, and improved upwelling indices for the U.S. West coast. *Journal of Geophysical Research: Oceans*, *123*(10), 7332–7350. https://doi.org/10.1029/2018jc014187

Jones, P. D., Jonsson, T., & Wheeler, D. (1997). Extension to the North Atlantic oscillation using early instrumental pressure observations from Gibraltar and south-west Iceland. *International Journal of Climatology*, *17*(13), 1433–1450. https://doi.org/10.1002/(sici)1097-0088(19971115)17:13<1433::aid-joc203>3.0.co;2-P

Kanamitsu, M., Ebisuzaki, W., Woollen, J., Yang, S.-K., Hnilo, J. J., Fiorino, M., & Potter, G. L. (2002). NCEP–DOE AMIP-II reanalysis (R-2). *Bulletin of the American Meteorological Society*, *83*(11), 1631–1644. https://doi.org/10.1175/bams-83-11-1631

Marrero-Betancort, N., Marcello, J., Rodríguez Esparragón, D., & Hernández-León, S. (2020). Wind variability in the Canary Current during the last 70 years. *Ocean Science*, *16*(4), 951–963. https://doi.org/10.5194/os-16-951-2020

Martin, E. R., & Thorncroft, C. D. (2014). The impact of the AMO on the West African monsoon annual cycle. *Quarterly Journal of the Royal Meteorological Society*, *140*(678), 31–46. https://doi.org/10.1002/qj.2107

McGregor, H. V., Dima, M., Fischer, H. W., & Mulitza, S. (2007). Rapid 20th-century increase in coastal upwelling off Northwest Africa. *Science*, *315*(5812), 637–639. https://doi.org/10.1126/science.1134839

Mohino, E., Janicot, S., & Bader, J. (2011). Sahel rainfall and decadal to multi-decadal sea surface temperature variability. *Climate Dynamics*, *37*(3–4), 419–440. https://doi.org/10.1007/s00382-010-0867-2

Mote, P. W., & Mantua, N. J. (2002). Coastal upwelling in a warmer future. *Geophysical Research Letters*, *29*(23), 5353–6154. https://doi.org/10.1029/2002gl016086

Narayan, N., Paul, A., Mulitza, S., & Schulz, M. (2010). Trends in coastal upwelling intensity during the late 20th century. *Ocean Science*, *6*(3), 815–823. https://doi.org/10.5194/os-6-815-2010

Pardo, P., Padín, X., Gilcoto, M., Farina-Busto, L., & Pérez, F. (2011). Evolution of upwelling systems coupled to the long-term variability in sea surface temperature and Ekman transport. *Climate Research*, *48*(2), 231–246. https://doi.org/10.3354/cr00989

Santos, F., deCastro, M., Gómez-Gesteira, M., & Álvarez, I. (2012). Differences in coastal and oceanic SST warming rates along the Canary upwelling ecosystem from 1982 to 2010. *Continental Shelf Research*, *47*, 1–6. https://doi.org/10.1016/j.csr.2012.07.023

Soares, P. M. M., Lima, D. C. A., Semedo, A., Cardoso, R. M., Cabos, W., & Sein, D. V. (2019). Assessing the climate change impact on the North African offshore surface wind and coastal low-level jet using coupled and uncoupled regional climate simulations. *Climate Dynamics*, *52*(11), 7111–7132. https://doi.org/10.1007/s00382-018-4565-9

Sousa, M. C., Alvarez, I., deCastro, M., Gomez-Gesteira, M., & Dias, J. M. (2017). Seasonality of coastal upwelling trends under future warming scenarios along the southern limit of the canary upwelling system. *Progress in Oceanography*, *153*, 16–23. https://doi.org/10.1016/j.pocean.2017.04.002

Sydeman, W. J., García-Reyes, M., Schoeman, D. S., Rykaczewski, R. R., Thompson, S. A., Black, B. A., & Bograd, S. J. (2014). Climate change and wind intensification in coastal upwelling ecosystems. *Science*, *345*(6192), 77–80. https://doi.org/10.1126/science.1251635

Sylla, A., Mignot, J., Capet, X., & Gaye, A. T. (2019). Weakening of the Senegalo–Mauritanian upwelling system under climate change. *Climate Dynamics*, *53*(7–8), 4447–4473. https://doi.org/10.1007/s00382-019-04797-y

Thomas, B. R., Kent, E. C., Swail, V. R., & Berry, D. I. (2008). Trends in ship wind speeds adjusted for observation method and height. *International Journal of Climatology*, *28*(6), 747–763. https://doi.org/10.1002/joc.1570

Wang, D., Gouhier, T. C., Menge, B. A., & Ganguly, A. R. (2015). Intensification and spatial homogenization of coastal upwelling under climate change. *Nature*, *518*(7539), 390–394. https://doi.org/10.1038/nature14235

Wohland, J., Omrani, N., Witthaut, D., & Keenlyside, N. S. (2019). Inconsistent wind speed trends in current twentieth century reanalyses. *Journal of Geophysical Research: Atmospheres*, *124*(4), 1931–1940. https://doi.org/10.1029/2018jd030083